Fluctuation and distribution of macroscopic order in formation processes of a dissipative structure

Shoichi Kai, Shigenori Wakabayashi, and Masahide Imasaki
Department of Electrical Engineering, Kyushu Institute of Technology, Tobata, Kitakyushu, 804, Japan
(Received 22 April 1985; revised manuscript received 7 October 1985)

We report the temporal developments of the variance and distribution of fluctuations of macroscopic order in a structure-formation process using an electrohydrodynamic instability of a nematic liquid crystal at $f > f_c$, where f and f_c are the applied and the critical field frequencies separating two different instabilities: a convective flow instability and a forced oscillatory instability of the director. At $f > f_c$, the dissipative structure appears essentially as the forced oscillatory instability of the director in a three-dimensional pattern in space. The temporal development of the variance is qualitatively in good agreement with the result expected from the noisy Landau equation for the early stage, which resembles the result in a transient process of laser radiation, theoretically and experimentally studied by Arecchi and Degiorgio, but not for the late stage. This comes from the spatial inhomogeneity of the macroscopic order. The distributions of the macroscopic order fluctuation have profiles similar to the Gaussian type (or lognormal type in the presence of externally applied noise) for the early stage, and have an asymmetric profile with negative skewness for the late stage. This would suggest that the growth process of the dissipative structure for the late stage is dominated by totally different kinetics from that for the initial stage.

I. INTRODUCTION

Transient phenomena near an instability point have been studied in various fields, such as hydrodynamic instabilities,[1,2] phase separation,[3-5] and oscillatory instabilities in an electrical circuit[6] and in laser radiation.[7] The former two (hydrodynamic instabilities and phase separation) have spatial degrees of freedom, but the latter do not. One statistical theory for such transient phenomena without spatial degrees of freedom is the laser-radiation theory of Arecchi and Degiorgio, which describes their experimental results[7] well. Another such theory is Suzuki's scaling theory,[8] which can describe the kinetics for all stages of the latter examples. We are, however, interested in the transient kinetics of the systems with spatial degrees of freedom.[1] One well-investigated example is the phase-separation process, which is a transient phenomenon in a process going from nonequilibrium to equilibrium.[3] Recently a large increase of electrical fluctuations was observed during a process of crystallization from supercooled liquid glycerol,[4] which is similar to the transient phenomena in laser radiation and in the present study. An idea given for the separation process therefore might extensively be applied to other systems with spatial degrees of freedom.

Dynamics in systems with spatial degrees of freedom, on the other hand, is classified into two different cases according to the following equation:

$$\dot{y} = L(-i\nabla)^{\alpha}\left[-\frac{\delta\Phi(y)}{\delta y}\right], \tag{1}$$

where y and L are an order parameter and a transport coefficient, respectively, and $\Phi(y)$ is the potential

$$\Phi(y) = \tfrac{1}{2}a'y^2 - \tfrac{1}{4}b'y^4 - \tfrac{1}{2}(\nabla y)^2 . \tag{2}$$

Here the index $\alpha = 0$ for nonconserving systems such as order-disorder transitions, and $\alpha = 2$ for conserving systems such as spinodal decomposition in alloys and phase separations in solutions. Scaling properties therefore strongly depend on the conservation law of the system.[3,9]

Phase-separation processes start as nucleation or spinodal decomposition, due to a first-order kinetics from a homogeneous state. At late stages, the inhomogeneity of the system becomes important since phase separation proceeds, and the interaction among local ordered phases in different locations appears, for example, through the diffusion process in the conserving system.[3,9,10] In this situation, the interfacial motions of ordered phases play an important role and therefore the kinetics and scaling laws in space and time are different from those for the early stage.[9,11-13] Such evidence has recently been observed in several systems, but details are still unknown.

Similar order-formation processes are observed in dissipative structure formations far from equilibrium. In Bénard-Rayleigh (BR) convection, wave-front motion and defect dynamics in convective rolls dominate growth in the late stage. The effects of defect dynamics are particularly important in the long-time behavior near steady state.[1,2,14,15] The dynamics of defects, such as the combining, climbing, and gliding, corresponds to a type of aging process, and the Burgers vector of defects is conserved in a system with a sufficiently large aspect ratio Γ. An isolated defect, however, can survive in a system with small Γ.[2,15] Therefore the Burgers vector is not conserved in this case. The model used for phase separation therefore may be useful to understand qualitatively the kinetics of the instability far from equilibrium in a system with

 ©1986 The American Physical Society

large Γ. From this point of view, we study a macroscopic pattern-formation process for the forced parametric oscillation of the director in the electrohydrodynamic (EHD) instability of a nematic liquid crystal and report the temporal growths of the variance and order fluctuation. In EHD, the characteristic time is much shorter than that in BR convection, typically by 2 or 3 orders of magnitude,[16] which is one of the advantages to investigating this subject.

A nonlinear macrodynamics for the EHD may approximately be described by the equation[17]

$$\dot{y}=a(\epsilon)y-by^3+\nabla^2 y+\xi(t)y+\eta(t) \tag{3}$$

for small ϵ $[=(V^2-V_c^2)/V_c^2]$, the normalized value of the deviation from the instability point V_c (the critical applied voltage). Here y, $\xi(t)$, and $\eta(t)$ are the macroscopic variable, an external noise voltage, and an internal thermal fluctuation, respectively. When the noise of the electric field is externally applied to the system, it shows properties of a multiplicative stochastic process.[18] This process leads to a nontrivial threshold shift onto the background shift due to a part $\bar{\xi}^2(t)$ of the external noise contained in $a(\epsilon)$.[19,20] This equation shows that the system is nonconserving. Equation (3) will not be valid for defect dynamics, which often appears in late stages of the development. In order to describe the late-stage dynamics (defect dynamics), a new equation is needed, which would be obtained under further consideration of Eq. (3) associated with the defect motions.[2] At this moment, therefore, the temporal stage valid for Eq. (3) is still unclear.

In EHD there are two different regimes distinguished by the space-charge relaxation time τ_σ (an inverse of a certain critical frequency f_c^{-1}): a dielectric and conductive regime.[16,21] Convective flow appears in the conductive regime, at sufficiently low applied frequency $f<f_c$, for which the space charge can sufficiently vary with the temporal variations of the external field. Then the director angle is a stationary order parameter and the space charge becomes an oscillatory order parameter with a spatially macroscopic structure, as in BR convection.[16,21–23] Many investigations have been done on this state in EHD. For example, from the same point of view, very recently Tsuchiya and Horie[24] experimentally showed the temporal evolution of a convective roll pattern in EHD of nematic liquid crystals. They also found an anomalous increase of fluctuation around the order parameter during the transient process. Because of the relatively low quality of the resolutions, no detailed discussion of the distribution profile was given.

On the other hand, when $f>f_c$, the director oscillates with spatial structure instead of oscillating with space charge because it cannot respond; this is the so-called forced parametric oscillation of the director.[21–23] In this case, the amplitude of the oscillation increases with the amount of space charge as long as the deviation from the instability point is very small.[21] Therefore, we can predict the formation process of the macroscopic order from the growth of the director oscillations. In this case, the characteristic length scale of the spatial structure is very small compared to the layer thickness, so that the phenomenon occurs basically in three dimensions. The advantage in using the dielectric regime is that many repetitions of the formation process can be easily obtained for short periods because the growth rate is very large. Therefore, a large number of samplings is possible; this is necessary to obtain the precise variance and a well-defined distribution. We find that the temporal change of the variance is in good agreement with theory for a homogeneous one-variable system in the early stage, but not in the late stage. This may be due to the inhomogeneity of the system at the late stage. The transient profile of the distribution changes from a Gaussian type for the early stage to an asymmetrically modified profile with a negative skewness for the late stage in the absence of external noise. When an external Gaussian white noise is superimposed on the system, the distribution changes from a log-normal profile (positive skewness) for the early stage to a profile with a negative skewness for the relatively late stage, but not for the steady state, which somewhat resembles a Lifshitz-Slyozov-Wagner-type distribution.[10]

II. EXPERIMENTAL SETUP

The sample used in the present study was the nematic liquid crystal MBBA (*n*-*p*-methoxybenzylidene-*p*-butylaniline), which was enclosed between two SnO_2-coated glass plates, as transparent electrodes, separated by polymer spacers (Mylar films, Mitsubishi Chemical Co.). The thickness d of the cell and the area S of electrodes were 108 ± 5 μm and 6×6 mm^2, respectively. The aspect ratio Γ, therefore, was about 55. Since the enclosed area was 10×10 mm^2, the lateral wall was liquid crystal, that is, it had not a rigid but a free lateral boundary. The temperature was controlled at $T=22.5\pm0.05$ °C using a copper container with a double wall. We have used a rubbing procedure to obtain homogeneous alignment. The critical voltage V_c for the convective pattern, the so-called Williams domains, was 9.05 V for a sinusoidal wave with frequency $f=60$ Hz. The critical frequency f_c separating the conduction regime (appearing as convective flow) from the dielectric regime (the forced oscillation of the director) was 85 Hz. The present experiment was done in the dielectric regime at $f=100$ Hz, where V_c, the threshold field for the oscillation, was 231 V. The electric field was applied with burstlike repetition with 1024 bursts for a fixed ϵ $[=(V^2-V_c^2)/V_c^2]$ as shown in Fig. 1. The phase of the applied field for each burst was always the same, i.e., the amplitude of a sinusoidal wave at time t_{0i} of the

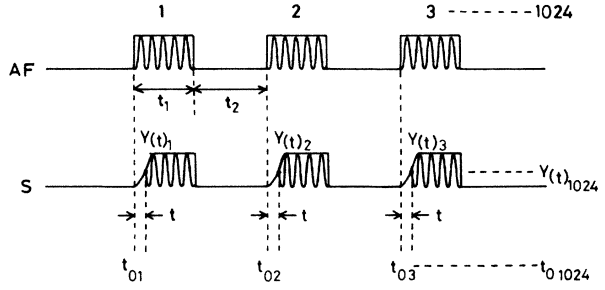

FIG. 1. Applied burst signal. AF denotes the applied field and S the response signal to AF.

ith pulse is always zero, which is controlled by a one-chip computer. Furthermore, a burst width t_1 was varied with ϵ, and the period t_2 chosen as the time to recover completely from the modified state to the initially uniform state. Here t_1 and t_2 are typically ~ 1 and ~ 30 sec at $\epsilon \sim 0.1$, respectively. As there was a small aging effect, i.e., a slight shift of V_c, we determined V_c and ϵ for each experiment. A single-mode He-Ne laser ($\lambda = 6328$ Å, 3 mW) and photodiode (NEC Co. LSD-39A) were used as an incident light source and as a detector, respectively. The diameter of the observation area was about 10 μm.

Signals from the photodiode were analyzed on a personal computer (NEC PC8001 and PC8011) after analog-to-digital conversion in eight bits with a sampling rate of 3.2 kHz. The experimental setup used in the present study is shown in Fig. 2.

The development of the oscillation was obtained from the envelopes of the oscillatory signal detected. The repetitions of the burst numbered 1024 and the temporal development of each envelope from t_{0i} to the steady state was obtained. Then the most probable path (mean formation route of the local order) was defined as the averaged route for all envelopes. Describing such averaged behaviors of the local order in space, there are two ways to obtain an averaged value: $\bar{y}_0$ at a fixed time,

$$\bar{y}_0(t^j) = \frac{1}{N} \sum_i^N y_i^j \quad \text{at } t^j , \tag{4}$$

and y_t at an averaged time $\bar{t}_0$,

$$\bar{t}_0(y_t^j) = \frac{1}{N} \sum_i^N t_i^j \quad \text{at fixed } y_t^j , \tag{5}$$

where N is 1024. Therefore, mean paths for both cases in Eqs. (4) and (5) are $\bar{y}_0(t)$ and $y(\bar{t}_0)$, The variance is given by

$$\sigma_0(t^j) = \frac{1}{N} \sum_i^N (\bar{y}_0 - y_i)^2 \quad \text{for } t^j . \tag{6}$$

In addition, to study the multiplicative stochastic properties we also superimposed external Gaussian white noise with the deterministic voltage using a noise generator (N.F. Co. WG-722) with a bandwidth of 5 kHz and a correlation time of 29.5 μsec. The intensity of the noise was determined as the magnitude of $\tau' = 0$ of the autocorrelation $\langle \xi(\tau')\xi(0) \rangle$ of the electrically applied noise $\xi(t)$, obtained from a signal analyzer (Iwatsu SM-2100A), which can calculate the autocorrelation and power spectrum directly from the signal.

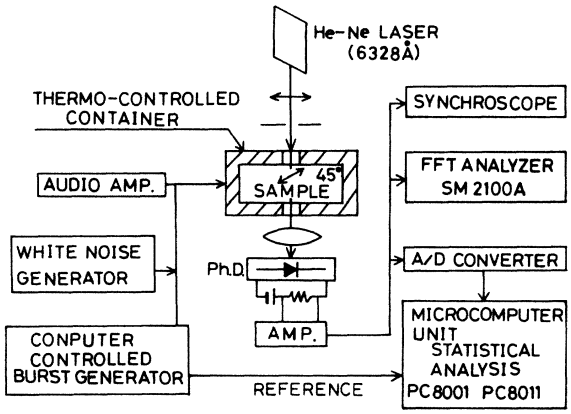

FIG. 2. Experimental setup.

III. RESULTS AND DISCUSSIONS

A. Developments and fluctuation of the director oscillation

Since the liquid crystal MBBA used has negative dielectric anisotropy, the director becomes oriented normal to the electric field which is parallel to the conductive glass plate, as shown in Fig. 3(a). With no space charge in the x direction, the director becomes aligned normal to the externally applied field $\mathbf{E}_z(t)$.[21-23] When the space charge is stored in the x direction due to the conductive anisotropy,[22] the lateral electric field $\mathbf{E}_x(t)$ develops, as shown in Fig. 3(b). Then the director is inclined to the direction normal of the composite electric field $\mathbf{E}$ ($=\mathbf{E}_z + \mathbf{E}_x$) with an angle θ to the glass plate.[23] Here, since $|\mathbf{E}_z| \gg |\mathbf{E}_x|$ in general, $|\mathbf{E}_x| = |\mathbf{E}| \sin\theta \sim |\mathbf{E}_z|\theta$ where $|\mathbf{E}_z|$ is the amplitude of the externally applied field.[21-23] Accordingly, the amplitude of θ is approximately proportional to the amplitude of the field $\mathbf{E}_x$ caused by the stored space charge [$q = (1/4\pi)(\text{div}\mathbf{D})$] for small ϵ (i.e., small θ). In fact, θ is found to be less than about 0.1 rad in our experiment. Reversing the external field ($\mathbf{E}_z$), the director again becomes aligned in the direction normal to $\mathbf{E}$ having an angle $-\theta$ as shown in Fig. 3(c), because the space charge is insensitive to $f > f_c$. (Naturally, in order to discuss more quantitatively on this dynamics we have to consider elastic and hydrodynamic effects.)[21-23]

Thus the amount of space charge determines the amplitude of the director oscillation.[21,22] This can be qualitatively understood from the theory for EHD.[21-23] The intensity change $\Delta I(t)$ of the light detected is approximately proportional to θ^2 (θ is the angle defined by the director and the glass plate) through the dielectric anisotropy of liquid crystal, and the amplitude y of the space charge with spatially periodic structure may also be proportional

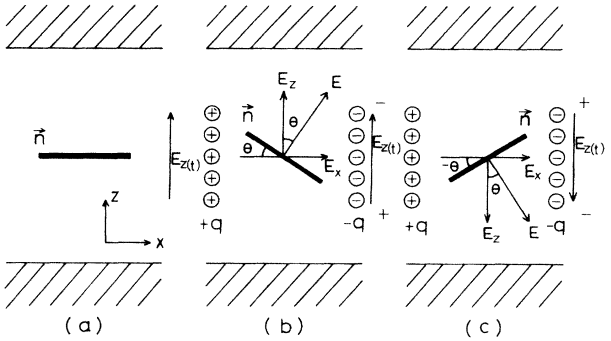

FIG. 3. The forced director oscillation due to the spatially stored charge by the applied field. (a) No space charge; (b) and (c), the dynamical behavior of the director when the sinusoidal electric field E_z is applied under the space charge stored with a periodic structure in the system.

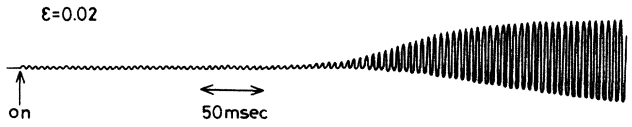

FIG. 4. Signal of the light intensity detected without summation.

to $[\Delta I(t)]^{1/2}$ since $\theta \propto y$ when the external parameter ϵ is very close to zero.[23] We regard, therefore, $[\Delta I(t)]^{1/2}$ as an order parameter y in Eq. (3). At relatively large ϵ, the interrelations will be much more complicated and accordingly we have restricted our discussions only to situations with very small ϵ.

A oscillatory signal caused by the director oscillation is optically observed at $f > f_c$ as shown in Fig. 4. This is generated by an inhomogeneous storage of space charges, and therefore the amplitude of the oscillation increases with an increase in the magnitude of the space charge. In this situation, the envelope of the temporal growth of the oscillation is due to an increase of the space charge.

In Fig. 5, the temporal development of the macroscopic order parameter y and the variance σ are shown in arbitrary units at $\epsilon=0.098$ when the external field is increased in a steplike fashion. Symbols $\bar{y}_0$, y_t, and σ_0 are defined in Eqs. (4)—(6). For fixed y_t, Eq. (5) is plotted as a function of $t=\bar{t}_0$ and $y_t(\bar{t}_0)$. The solid line in Fig. 5 shows the solution of the equation $\dot{y}=ay-by^3$ ($a=32.5$, $b=0.28$). In Fig. 5, $\bar{y}_0$, y_t, and σ_0 are normalized by the steady-state values y_∞, $y_{t\infty}$, and the maximum value σ_m, respectively. The experimental data for both $\bar{y}_0$ and y_t are well described by the equation $\dot{y}=ay-by^3$. σ_0 is the variance of the y distribution at a fixed time, as described in Eq. (6). $\sigma_0(t)$ shows the maximum value σ_m at $t=t_m > t_{1/2}$, the time at which y assumes half the value of y_∞. Then $\sigma_0(t)$ decreases, tending to the steady state of the system. The solid line shows a fluctuation-enhanced theory for $\dot{y}=ay-by^3+\eta(t)$,[25]

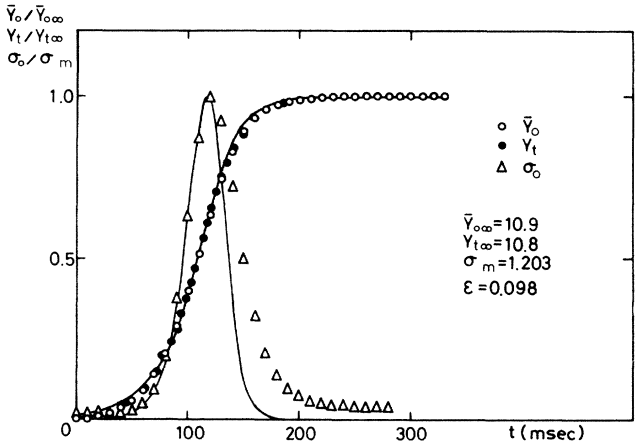

FIG. 5. Temporal development of the macroscopic order y and variance σ at $\epsilon=0.098$. $\bar{y}_0(t)$, the mean value for a fixed t; $y_t(\bar{t}_0)$, the macroscopic value for the mean time $\bar{t}_0$; σ_0, the variance around the $\bar{y}_0$. The solid line for σ_0 shows Eq. (7).

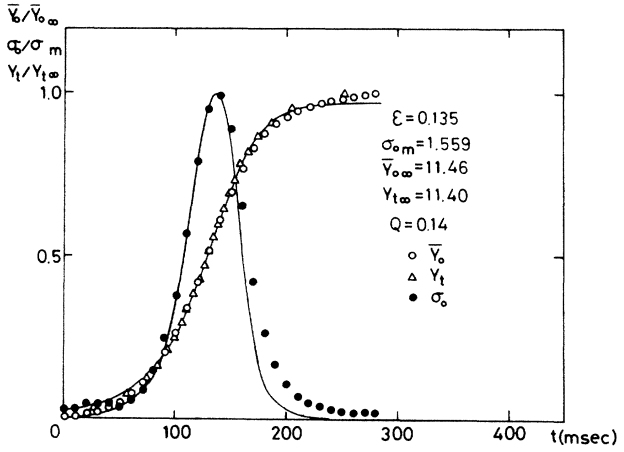

FIG. 6. Temporal development of the macroscopic order y and the variance σ at $\epsilon=0.135$ with white noise $Q=0.14$. The solid lines for σ_0 and for $\bar{y}_0$ and y_t indicate Eqs. (7) and (3) with $a=27$ and $b=0.22$ neglecting other terms in Eq. (3), respectively.

$$\sigma_0 \propto \left[\frac{\dot{y}(t)}{y(0)}\right]^2 = A\frac{\exp(2at)}{[\exp(2at)+\delta]^3}\ , \tag{7}$$

where A and δ are constants related to the steady state and the initial values of σ and y. For $t < t_m$, the agreement between the theoretical curve and the experimental data is quite good, but not for $t \gtrsim t_m$. This deviation increases as the steady-state is approached.

When white noise is externally superimposed on the system, the formation process is slightly changed. Figure 6 shows the result at $\epsilon=0.135$ and $Q=0.14$, where Q is the ratio of the white-noise intensity and the amplitude of the deterministic electric field. There is no qualitative difference. White noise seems to delay the formation of macroscopic order, as predicted by a multiplicative stochastic process.[18] However, in EHD, the system may also behave at small Q and small ϵ as an additive noise process, since $\xi y \ll \eta$ in Eq. (3). Figure 7 shows the white-noise effect on σ_0 at $\epsilon=0.135$. The maximum value of σ_0 becomes four times larger with the external noise than

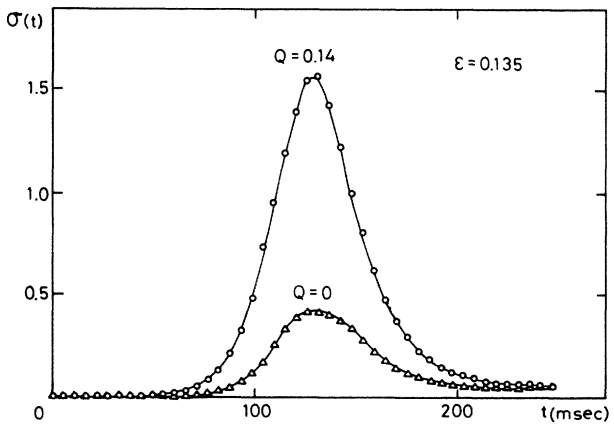

FIG. 7. The effect of white noise on the variance σ.

that without; namely, the white noise enhances fluctuations in the system. The time t_m, however, is not influenced greatly by the white noise and is almost the same in both cases.

B. Distribution of fluctuations around the most probable path $\bar{y}_0$

Figure 8 shows temporal developments of the distribution of fluctuations around $\bar{y}_0$ at $\epsilon=0.067$ and $Q=0$. The qualitative features resemble those observed by Tsuchiya and Horie.[24] As seen in Fig. 8(a), the distributions change clearly near t_m. Namely, we note that the distribution profiles for the early stage and for the steady state are very sharp and similar but they are quite different from those for the transient region where the large growth rate occurs. This tendency is the same for all experimental results at small ϵ. In the case without an external noise, the distribution has a Gaussian profile for the early stage at $t=109$ msec [Fig. 8(b); $\tau=t/t_m=0.484$], but the deviation from the Gaussian profile increases with time [see Fig. 8(c)]. The distribu-

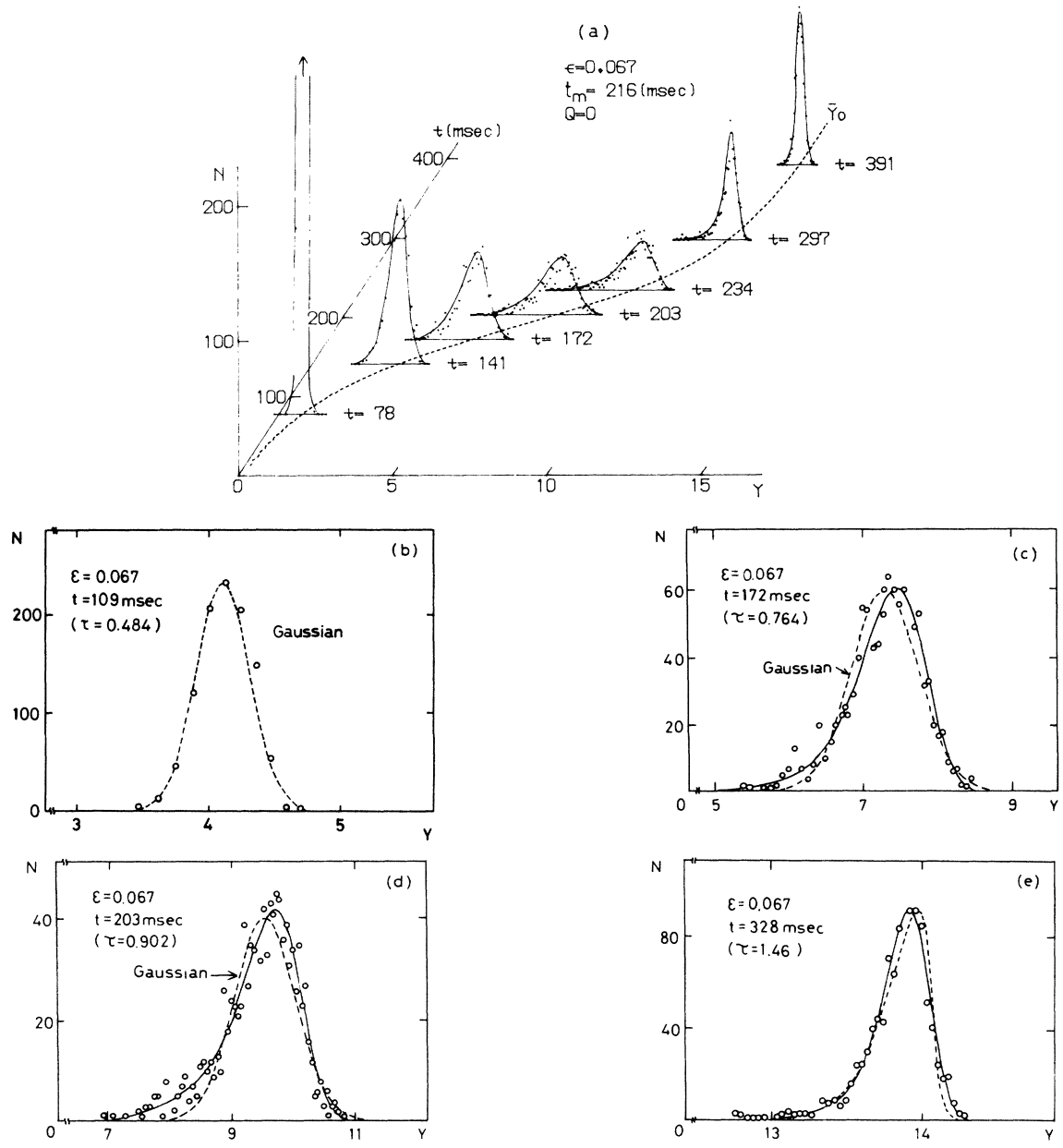

FIG. 8. Temporal developments of the distribution around $\bar{y}_0$ at $\epsilon=0.067$. The fitting function used here is $N(y;N_m,\bar{y}_0,\sigma_G,s,f)=N_m\exp\{-[(y-\bar{y}_0)^2/2\sigma_G-(y-\bar{y}_0)^3/6s+(y-\bar{y}_0)^4/24f]\}$. (a) Development from $t=0$ to the steady state. (b) $t=109$ msec, $\tau=t/t_m=0.484$: dotted line, $\sigma_G=0.0441$. (c) $t=172$ msec, $\tau=0.764$: dotted line, $\sigma_G=0.203$; solid line, $N_m=61.12$, $\bar{y}_0=7.44$, $\sigma_G=0.185$, $s=-0.128$, and $f=0.18$. (d) $t=203$ msec, $\tau=0.902$: dotted line, $\sigma_G=0.25$; solid line, $N_m=42.5$, $\bar{y}_0=9.7$, $\sigma=0.23$, $s=-0.35$, and $f=0.165$. (e) $t=328$ msec, $\tau=1.46$. The dotted line and the solid line in (e) show the classical LSW distributions (Ref. 9) and the best-fitted curve with $N_m=91$, $\bar{y}_0=13.92$, $\sigma_G=0.023$, $s=-0.0054$, and $f=0.0031$, respectively.

tion beyond t_m becomes asymmetric with negative skewness as shown in Figs. 8(d) and 8(e). This tendency with negative skewness is seen especially clearly at $0.8 \lesssim \tau \lesssim 1.4$, where nonlinear effects and mode selection of macroscopic order probably becomes important.

When $Q=0.14$, the distribution has positive skewness and is well fitted for the initial stage [$t=109$ msec; Fig. 9(a)] with a lognormal profile. The lognormal distribution[26]

$$N(y)=(N_0\bar{y}_0/y)\exp\{-[\ln(y/\bar{y}_0)]^2/2\sigma^2\} \quad (8)$$

is often observed in statistical properties of the variable y, which has the multiplicative relation $y_{n+1}=y_nP$, where P is a random coefficient. Here $\bar{y}_0$ is the mean value.

The distribution becomes, however, Gaussian near t_m and then changes into a distribution with negative skewness, also shown in Figs. 9(b)—9(d). These tendencies of the distribution profile are qualitatively the same for $0.04<\epsilon<0.15$ and $Q<0.15$, regardless of ϵ and noise intensity Q. For the steady state the distribution has a sharp peak again, and therefore it is difficult to say whether it is Gaussian or another type.

We also examined a fit with a Lifshitz-Slyozov-Wagner (LSW) type of distribution which appears in a polydisperse crystal-growth process controlled by diffusion from the point of view described in Sec. I. For late stages, the distribution seems to be rather well fitted with the LSW-type profile [see Fig. 9(d)].

C. Discussion

We summarize the results obtained here as follows.

(1) The variance σ_0 has a maximum value σ_m at $t=t_m$, then decreases.

(2) The temporal change of σ_0 for $t<t_m$ can be described by the noisy Landau equation $\dot{y}=ay-by^3+\eta(t)$.

(3) The distribution around $\bar{y}_0$ is Gaussian for $t \ll t_m$, but becomes one with negative skewness nearing t_m ($\sim t>0.8t_m$).

(4) When external noise is applied, the distribution for the early stage is well fitted to the lognormal one, then for $t \sim t_m$ it becomes Gaussian, and for the late stage the distribution has negative skewness.

The deviation of σ_0 from Eq. (7) increases for the later stage $t>t_m$ as shown in Fig. 5. In Eq. (7), spatial degrees of freedom and externally applied noise effects are not taken into account. It may be considered, therefore, that the theory without the term $\nabla^2 y$ holds for the early stage but not for the late stage because the inhomogeneity of the

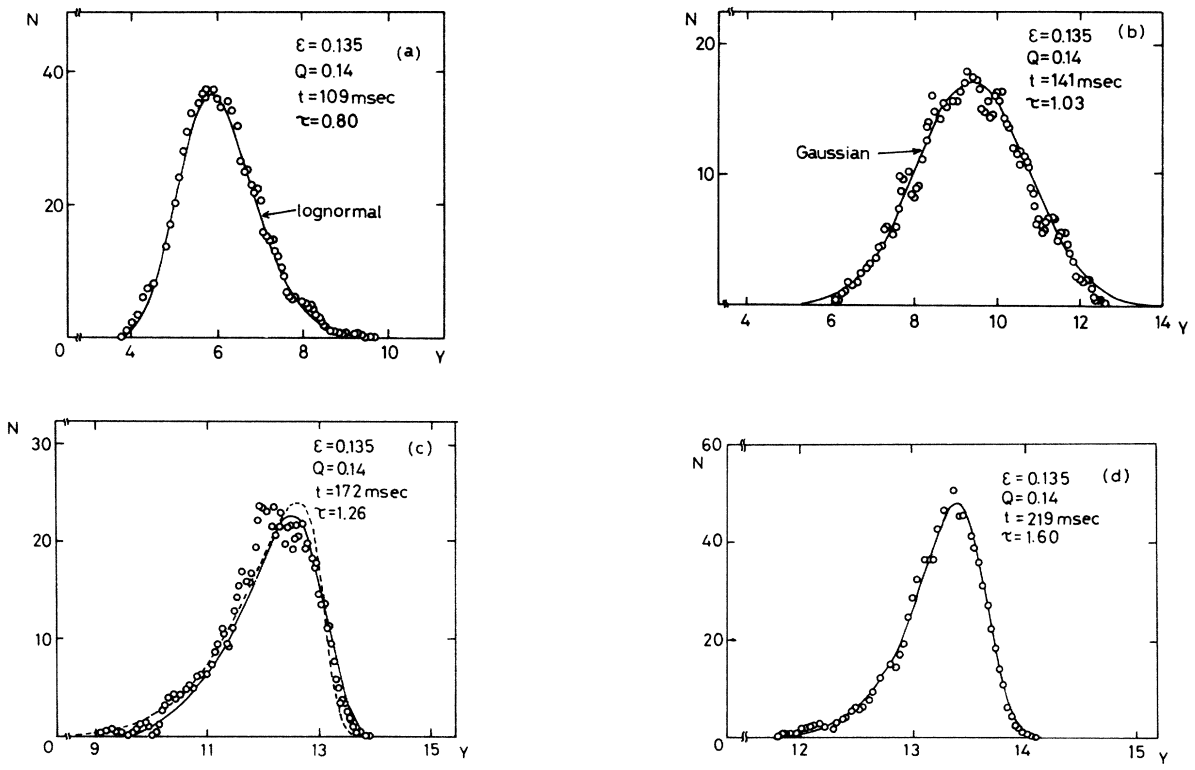

FIG. 9. Temporal developments of the distribution around $\bar{y}_0$ at $\epsilon=0.135$ with $Q=0.14$ (in this figure, each data point is plotted after averaging by each of the five neighboring points, i.e., the smoothing is done). (a) $t=109$ msec, solid line shows the lognormal distribution with $\sigma=0.02$, $\bar{y}_0=6.2$, and $N=38$. Here $\bar{y}_0$ is not exactly the same as y_m at the maximum of the distribution as is well-known for the lognormal distribution (Ref. 28). (b) $t=141$ msec ($\tau=1.03$): solid line shows the Gaussian distribution with $\sigma_G=1.823$. (c) $t=172$ msec ($\tau=1.26$): solid line, $N_m=22.8$, $\bar{y}_0=12.55$, $\sigma_G=0.45$, $s=-0.30$, and $f=0.35$; dotted line, the classical LSW distribution (Ref. 9). (d) $t=219$ msec ($\tau=1.60$): solid line, $N_m=48$, $\bar{y}_0=13.38$, $\sigma_G=0.088$, and $s=-0.032$, and $f=0.022$.

macroscopic order plays an important role in Eq. (3) for a system with spatial degrees of freedom. In addition, many defects are usually produced at boundaries of domains having different growth stages in space, where the kinetics must be different from Eq. (3), as mentioned in the Introduction. This often shows long-time transient behavior for $t \gg t_m$.

On the other hand, the behavior of σ_0 and t_m in the presence of external noise is related to the multiplicative stochastic process. It can be said that externally applied noise rather strongly affects the early stage, according to the distribution profile (the lognormal type). Once the order is formed, external noise is relatively ineffective. This can be seen clearly in the distribution profiles obtained here.

Thus it may be said that the growth process of macroscopic order for the late stage is clearly different from that for the early stage both with and without external noise.

Figure 10 schematically illustrates one of the qualitative reasons for the increase in σ_0. Throughout the development of the system to the steady state, there are various paths $y_1, y_2, \ldots, y_n$ depending on initial fluctuations as shown in Fig. 10(a). By repeating the measurements many times, the frequency distribution of the paths may be obtained around the most probable path and the temporal change of σ_0 may also be thereby obtained [Fig. 10(b)]. At $t = t_m$, the deviation between the fastest growth y_1 and the slowest one y_n becomes maximum; that is, $\sigma = \sigma_m$. This is a qualitative explanation with no spatial information and cannot give us the interpretation of the characteristic deviation from Eq. (7) observed for the late stage. The result may be regarded as the deviation of local growth processes in space, and the distribution may correspond to one of the spatial inhomogeneities

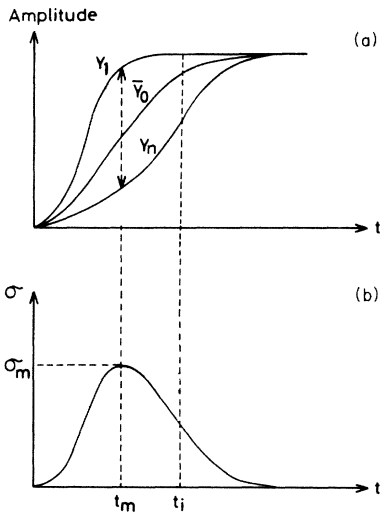

FIG. 10. Schematic illustration of the growth process (y) and the variance (σ) as a function of time. (a) $\bar{y}_0$, the most probable path (the averaged route); y_1, the fastest growing path; y_n, the slowest growing path. At the fixed time t_1, the order $y(t_1)$ on the path y_i is in a later stage of growth than that on the y_{i+1}. (b) σ_m, the maximum variance (the maximum deviation among paths).

of local growth in macroscopic order for $t \geq t_m$. On boundaries, in fact, many defects are produced and canceled by the competition of growth of the bulks or by climbing and gliding on the walls. This would be another origin of the anomaly by σ_0. We must take defect dynamics into account there.

Considering what we have described above, we might speculate as follows. The state at $t < t_m$ is considered the nucleation process, resulting in many nuclei of the macroscopic order. Those nuclei of macroscopic order have already grown over the whole area at $t \sim t_m$, although each one is in a different growth stage in space. Since interfaces among them cause the production of many defects, interaction among local orders takes place and some of them grow and others decay. This corresponds to an aging process, which results in a spatially homogeneous pattern through defect kinetics. In this stage, Eq. (3) may no longer be valid, and a new kinetic equation would be needed. In other words, using terminology and similarity of kinetics of a first-order phase transition, for example, such as a droplet growth process from a vapor phase, at $t \sim t_m$ the nucleation process is already completely finished (new nuclei are not produced anymore). After that, each crystal nucleus grows larger and becomes a single crystal by the aging process during $t \gtrsim t_m$. In this period, the growth kinetics (macrodynamics) is different from the kinetics in the nucleation process. Namely, the interaction among macroscopic orders that are spatially dispersed inhomogeneously plays an important role for $t \gtrsim t_m$, similar to Ostwald aging.[10,27,28] The application of white noise produces large fluctuations (many modes) at $t < t_m$. At late stages ($t \geq t_m$), such fluctuations are canceled by each other through the aging process.

However, a precise analogy of kinetics between crystal (droplet) growth and the present order-formation processes cannot be made, because the conservation law is not the same in relation to Eq. (3) and the defect dynamics is unknown. Using the same viewpoint, we may be able to explain the white-noise effect on the distribution. No detailed investigation of multiplicative stochastic properties on Eq. (3), however, has been done. There is therefore no proper model of the appearance of the lognormal distribution in the early stage. In general, however, it has frequently been observed for a stochastic process with a multiplicative property, such as a cascade process, which could apply here. In either case, for the early stage, the growth kinetics in the presence of external noise is different from that in its absence. It is worth noting that a size distribution of crystal growth due to the second-order surface-controlled-growth (SOCG) kinetics has a similar profile to the lognormal one.[27,28] In addition, it is also worth noting that the distribution experimentally obtained for the late stage is well fitted with the LSW distribution.[10]

Described in a more general sense, it is as follows. There is no coupling among Fourier components of modes in the linear growth regime (the very early stage). For the late stage, however, coupling occurs because of the term y^3. When the system has spatial degrees of freedom, the spatial interaction of modes is produced through the term $\nabla^2 y$, especially for the late stage, contrary to the case with

no spatial degree of freedom. The difference, therefore, must be due to spatial inhomogeneity producing many domains and defects, i.e., growth of various spatial modes. Such modes, however, are removed by mode selection during the final stage after t_m. Namely, defects with opposite signs of Burgers vectors cancel each other and disappear. This is a growth process near the steady state. The growth for the late stage, therefore, must be closely related to the dynamics of defects.[2,14,15] It will then lead to a new macroscopic equation associated with defect dynamics. The Burgers vector of defects would be the new order parameter for this stage and would be conserved in large Γ. The present system is essentially in three dimensions, unlike the common BR convection system, since Γ is quite large (~ 55) and the structure is quite small ($\sim d/20$) comparing to the thickness d. For cells of identical thickness, large Γ leads to longer onset times (t_m); that is, lateral size, as well as thickness, also plays an important role in the present experiment. Therefore, we must also take into account the effect of the dimensionality.

IV. CONCLUSIONS

The temporal change of the variance in a dissipative structure formation for the early stage is in good agreement with the result expected from the noisy Landau equation as well as the result in the transient process of the laser radiation obtained by Arrechhi and Degiorgio.[7] However, it has a large deviation from theory for the late stage $t \gtrsim t_m$ when σ has the maximum value (σ_m). The evolution of the distribution has a tendency similar to that of $\sigma_0(t)$; namely, it changes with time, showing characteristic features. The distribution in the early stage with external noise is quite different from one without, and exhibits a lognormal profile. This suggests that the growth kinetics for the early stage is strongly influenced by the application of external noise. It is generally well known that lognormal distribution comes from a multiplicative process. This may be the case. For the late stage, however, its influence is not remarkable.

We have noted qualitatively an analogy between crystal (droplet) growth and a dissipative structure formation for the late stage in the present paper. Of course, there must be differences between kinetics of a first-order transition and of the instability in a dissipative structure. Although the validity for the similarity between the crystal growth and the macroscopic order-formation processes is not yet clear, we believe that the analogy of the concept given here may be valuable for future theoretical approaches.

Finally, we would like to stress that properties and kinetics at the late stage are clearly different from those at the early stage in dissipative structure formation processes. This difference originates from defect motions.

ACKNOWLEDGMENTS

The authors would like to thank Dr. H. R. Brand for his invaluable suggestions and comments. We also thank Professor K. Kawasaki, Professor T. Yamada, and Professor H. Furukawa for valuable discussions and for focusing their interests on the present work. This work was partially supported by the Grant-in-Aid for Special Project Research from the Ministry of Education, Science, and Culture and by Yamada Science Foundation.

[1]L. Kramer, E. B. Jacob, H. R. Brand, and M. C. Cross, Phys. Rev. Lett. **49**, 1891 (1982); G. Dee and J. S. Langer, *ibid.* **50**, 383 (1983).

[2]For example, H. S. Greenside and W. M. Coughran, Jr., Phys. Rev. A **30**, 398 (1984); A. Pocheau and V. Croquette, J. Phys. (Paris) **45**, 35 (1984).

[3]J. D. Gunton, M. S. Miguel, and P. S. Sohni, *Phase Transitions and Critical Phenomena,* 8th ed., edited by C. Domb and J. L. Lebowitz (Academic, New York, 1983), and references therein.

[4]K. Tozaki and Y. Yamaguchi, J. Phys. Soc. Jpn. **53**, 1904 (1984).

[5]S. Komura, K. Osamura, H. Fujii, and T. Takeda, Phys. Rev. B **30**, 2944 (1984).

[6]S. Kabasima, M. Itsumi, T. Kawakubo, and T. Nagashima, J.Phys. Soc. Jpn. **39**, 1183 (1975).

[7]F. T. Arecchi and V. Degiorgio, Phys. Rev. A **3**, 1108 (1971).

[8]M. Suzuki, Adv. Chem. Phys. **46**, 195 (1981); Y. M. Wong and P. H. Meijer, Phys. Rev. A **26**, 611 (1982).

[9]T. Ohta, D. Jasnow, and K. Kawasaki, Phys. Rev. Lett. **49**, 1223 (1982); K. Kawasaki and T. Ohta, Physica **118A**, 175 (1983).

[10]I. M. Lifshitz and V. V. Slyozov, J. Phys. Chem. Solids **19**, 35 (1961).

[11]M. Tokuyama and K. Kawasaki, Physica **123A**, 386 (1984).

[12]H. Furukawa, Physica **123A**, 497 (1984).

[13]J. A. Marqusee and J. Ross, J. Chem. Phys. **80**, 386 (1984).

[14]P. Manneville, J. Phys. (Paris) **44**, 759 (1983).

[15]J. A. Whitehead, Phys. Fluids **26**, 2899 (1983).

[16]S. Kai and K. Hirakawa, Prog. Theor. Phys. Suppl. **64**, 212 (1978).

[17]For example, under a dc electric field without terms $\xi(t)y$, and $\eta(t)$, H. Hijikuro, Prog. Theor. Phys. **54**, 592 (1975).

[18]A. Schenzle and H. R. Brand, Phys. Rev. A **20**, 1628 (1979); W. Horsthemke and R. Lefever, *Noise-Induced Transitions* (Springer-Verlag, Berlin, 1984), pp. 164—189.

[19]S. Kai, T. Kai, M. Takata, and K. Hirakawa, J. Phys. Soc. Jpn. **47**, 1379 (1979).

[20]T. Kawakubo, A. Yanagita, and S. Kabashima, J. Phys. Soc. Jpn. **50**, 1451 (1981).

[21]I. W. Smith, Y. Galerne, S. T. Lagerwall, E. Dubois-Violette, and G. Durand, J. Phys. (Paris) Colloq. **36**, C1-237 (1975).

[22]W. Helfrich, J. Chem. Phys. **51**, 4092 (1969).

[23]P. G. de Gennes, *The Physics of Liquid Crystals,* 3rd ed. (Clarendon, Oxford, 1982).

[24]Y. Tsuchiya and S. Horie, J. Phys. Soc. Jpn. **54**, 1 (1985).

[25]R. Kubo, K. Matuo, and K. Kitahara, J. Stat. Phys. **9**, 51 (1973).

[26]J. Aitchison and J. A. C. Brown, *The Lognormal Distribution* (Cambridge University, Cambridge, England, 1957).
[27]M. Kahlweit, Adv. Colloid Inteface Sci. **5**, 1 (1975).
[28]H. H. Hohmann and M. Kahlweit, Ber. Bunsenges, Phys. Chem. **76**, 933 (1972) (we actually tried to fit their data in Fig. 2 of Ref. 28 with a lognormal distribution, which is rather better fitting than the SOCG which they did).